

# Broadening of the $QCD_3$ flux tube from the AdS/CFT correspondence

---

**Jeff Greensite**

*Physics and Astronomy Dept., San Francisco State University  
San Francisco, CA 94132 USA  
E-mail: greensit@quark.sfsu.edu*

**Poul Olesen**

*The Niels Bohr Institute, Blegdamsvej 17, DK-2100 Copenhagen Ø, Denmark  
E-mail: polesen@nbi.dk*

**ABSTRACT:** We use the finite temperature AdS/CFT approach to demonstrate logarithmic broadening of the confining  $QCD_3$  flux tube as a function of quark separation. This behavior indicates that, unlike lattice QCD, there is no roughening transition in the AdS/CFT formulation, which raises the interesting possibility of extrapolating strong coupling results to weak couplings by the use of resummation techniques. In the zero-temperature non-confining limit, we find that this logarithmic broadening of the field strength distribution is absent. Our results are obtained numerically at strong couplings, in the supergravity approximation.

**KEYWORDS:** Confinement, AdS-CFT Correspondence, Brane Dynamics in Gauge Theories.

---

## Contents

<b>1. Introduction</b>	<b>1</b>
<b>2. Equations of motion in the saddle-point approximation</b>	<b>3</b>
<b>3. Numerical Solution for the Minimal Surface</b>	<b>7</b>
<b>4. Analytic Approximation</b>	<b>14</b>
<b>5. Four dimensional QCD</b>	<b>17</b>
<b>6. Conclusions</b>	<b>17</b>

---

## 1. Introduction

Until recently, the analytical investigation of QCD at large distance scales was only possible in the framework of strong coupling lattice gauge theory. This formulation has many beautiful features, and the existence of confinement, chiral symmetry breaking, and a mass gap can be demonstrated in an elegant way. It was once hoped that these strong coupling results could be extrapolated to weaker couplings via Pade approximants, or by some other clever resummation method. These hopes were abandoned with the recognition that there exists a roughening transition in lattice gauge theory, which separates the strong and weak coupling phases. In the roughened phase, the QCD flux tube is believed (on the basis of some simple string arguments [1]) to broaden as the quark-antiquark pair are separated; the cross-sectional area of the flux tube should increase logarithmically with separation. In the strong-coupling phase, however, this broadening simply does not occur; the chromo-electric flux tube does not really behave like a quantized string. This unrealistic feature of strong-coupling lattice theory is a fundamental limitation, which prevents the use of strong coupling results to draw conclusions about physics in the continuum.

The AdS/CFT correspondence put forward by Maldacena [2] provides a new way of doing strong coupling calculations in large-N gauge theories with an ultraviolet cutoff. The effective cutoff is provided by a compactified Euclidean time variable, equivalent to a finite temperature, which supplies the required supersymmetry breaking [3]. As in lattice gauge theory, the existence of confinement and a mass gap can be elegantly demonstrated at strong couplings. On the other hand, as discussed by

Gross and Ooguri [4], the non-supersymmetric theory constructed in this way is really only equivalent to large  $N$  QCD in the limit where the temperature  $T$  goes to infinity and the coupling  $\lambda = g_{YM}^2 N$  approaches zero, with (in D=4 dimensions) [4]

$$T \rightarrow \infty \quad \text{and} \quad \lambda \rightarrow \frac{B}{\ln(T/\Lambda_{QCD})}, \quad (1.1)$$

where  $\Lambda_{QCD}$  is the QCD scale. The supergravity approximation clearly breaks down in these limits, where no results are presently available. The AdS/CFT approach is so far only tractable in the supergravity approximation, where the temperature  $T$  is an ultraviolet cutoff and  $\lambda \gg 1$  is the bare coupling at the scale  $T$ . Only in this strong coupling limit has the string tension has been computed, via a saddle-point approximation [5], and the low-lying glueball spectrum obtained. Some preliminary results in the one loop approximation are also available [6–8].

Since we are limited to strong couplings, it is interesting to ask how far the results extracted from the AdS/CFT correspondence agree with our expectations of large- $N$  QCD in the continuum. Further, we would like to know if there is any fundamental obstruction, as there is in lattice gauge theory, to extrapolating strong coupling AdS/CFT results to weaker couplings. In this article we will study one aspect of these issues, namely, the question of whether strongly-coupled QCD<sub>3</sub> is in the roughened phase in the AdS/CFT correspondence. The theory is in the rough phase, as explained many years ago by Lüscher, Münster, and Weisz [1], if the QCD flux tube broadens logarithmically with quark separation. If this logarithmic broadening, due to quantum vibrations of the flux tube, is *not* found at strong couplings, then there is likely to be a roughening transition between the strong and weak coupling regimes. As a consequence, information about the strong coupling phase could not be used to gain any insight in the physical weak coupling scaling limit.

Although the interquark potential is derived from a string theory in the AdS/CFT correspondence, the question of flux tube broadening by vibrations is non-trivial, since the potential is represented by a string theory in both the supersymmetric and non-supersymmetric gauge theories, while only the latter case would be expected to show logarithmic broadening. Moreover, our investigation will be limited to the saddle-point evaluation of loop-loop correlation functions, and vibrations around the saddle-point will not be considered. In view of this, the success of the AdS/CFT approach is noteworthy: We find, in the finite temperature case, that the width of the QCD flux tube already shows roughening in the saddle-point approximation, with the (width)<sup>2</sup> proportional to the logarithm of the interquark distance, as expected for *vibrating* strings [1], [9]. For the zero temperature case, where one has a conformal theory, this logarithmic broadening does not occur. The latter result is achieved in the AdS/CFT approach by a remarkable fine tuning of the relevant string worldsheet in the zero temperature case, which of course is related to the absence of

a horizon. Superficially the metric and the relevant saddle-point configuration look very similar to the  $T \neq 0$  case, but they nevertheless manage to produce, by subtle effects, a very different behavior. Thus, in the finite temperature case, the type IIB string in  $D = 10$  dimensions ( $AdS_5 \times S_5$ ) is associated with a confining flux tube of finite width in flat  $D = 3$  dimensional space, while in the zero-temperature case the superstring in 10 dimensions does not give rise to a flux tube of this kind.

The presence of roughening in the finite temperature case is interesting on several grounds. First, it adds to the list of successes of the strong-coupling AdS/CFT formulation, which include the existence of a linear interquark potential, a Lüscher  $1/R$  correction to that potential, a mass gap, and a quasi-realistic pattern of glueball mass-splittings.<sup>1</sup> Second, it demonstrates that there is unlikely to be a roughening transition between strong and weak coupling phases, and hence no obstruction (at least from this source) to extrapolating strong coupling expansions to weaker couplings by resummation methods. Finally, the AdS/CFT correspondence provides the first actual derivation of roughening in a non-abelian gauge theory, albeit at strong couplings. Previous arguments for roughening [1] were based on a string picture which was not derived from gauge theory, while numerical lattice simulations of non-abelian gauge theory have neither confirmed nor denied the existence of roughening. The flux tube width has in fact been studied numerically, but the relevant error bars are simply too large to draw definite conclusions.<sup>2</sup> All that can be said is that existing Monte Carlo data is compatible with logarithmic broadening of the flux tube, but it is also perfectly compatible with a constant width for the QCD flux tube [11].

## 2. Equations of motion in the saddle-point approximation

The color-electric energy density  $\mathcal{E}(x)$  of a flux tube running between static quark-antiquark sources is given by

$$\mathcal{E}(\mathbf{x}) \propto \langle q\bar{q} | \text{Tr} \vec{E}^2(\mathbf{x}) | q\bar{q} \rangle - \langle 0 | \text{Tr} \vec{E}^2 | 0 \rangle \quad (2.1)$$

where  $|q\bar{q}\rangle$  is the (normalized) ground state of the gluon field in the presence of the static  $q\bar{q}$  color sources, and  $|0\rangle$  is the ground state in the absence of static sources. If we are interested, in particular, in the energy density of the spatial component of the color electric field parallel to the axis of the flux tube, then this is given by the

---

<sup>1</sup>The existence of the Lüscher  $1/R$  term in the AdS/CFT correspondence now seems very plausible, c.f. ref. [7], although, as discussed in this reference, some ambiguities remain, and the precise coefficient of this term is still uncertain. The interpretation of the coupling-independent  $1/R$  term in the potential is also complicated by the fact that such a term also arises, in the AdS/CFT correspondence, in the zero-temperature non-confining limit [8, 12].

<sup>2</sup>Roughening has been observed in numerical simulations of one simple abelian model, namely,  $Z_2$  lattice gauge theory in  $D = 3$  dimensions [10]. But there is no evidence for or against this effect in any non-abelian model.

connected correlator of a large  $R \times T$  Wilson loop (denoted  $C_2$ ) with  $T \gg R$ , and a Wilson loop around a much smaller loop  $C_1$

$$\mathcal{E}_{||}(\mathbf{x}) \propto \frac{\langle \text{Tr}[U(C_1)]\text{Tr}[U(C_2)] \rangle - \langle \text{Tr}[U(C_1)] \rangle \langle \text{Tr}[U(C_2)] \rangle}{\langle \text{Tr}[U(C_2)] \rangle} \quad (2.2)$$

where  $C_1$  is parallel to the plane of the larger loop and centered at point  $\mathbf{x}, t = 0$ , and where  $\text{Tr}[U(C)]$  denotes the trace of the Wilson loop around contour  $C$ . Usually we are interested in the width of the flux tube in the plane equidistant between the static quark sources. If the quark and antiquark sources are located at spatial positions  $(0, 0, -R/2)$  and  $(0, 0, R/2)$ , respectively, then the width  $w_R$  of the  $QCD_4$  flux tube can be defined, e.g., by the quantity

$$w_R^2 \equiv \frac{\int dx_1 dx_2 (x_1^2 + x_2^2) \mathcal{E}_3(x_1, x_2, 0)}{\int dx_1 dx_2 \mathcal{E}_3(x_1, x_2, 0)} \quad (2.3)$$

The flux-tube width  $w_R$  is not very sensitive to the shape of loop  $C_2$ . Instead of a rectangular  $R \times T$  loop, one could use instead a circular loop of radius  $R$  in eq. (2.2); this corresponds physically to creation of a heavy quark-antiquark pair which move gradually apart to a maximum separation  $R$ , and then come gradually together again and annihilate. If the small loop  $C_1$  is concentric with loop  $C_2$ , at a transverse separation  $H$  as shown in Fig. 1, then the connected loop correlator measures the color-electric energy density of the flux tube at maximum quark separation  $R$ , at a transverse distance  $H$  from the midpoint of the axis of the flux tube.

The quantity  $w_R^2$  can be computed from a lattice strong coupling expansion. At strong couplings,  $w_R^2$  goes to a finite constant in the  $R \rightarrow \infty$  limit; i.e. the width of the flux tube is independent of the quark-antiquark separation at large  $R$ . However, it was shown many years ago in ref. [1] that  $w_\infty^2$  diverges at  $\beta \approx 1.9$ , for  $SU(2)$  lattice gauge theory in  $D = 4$  dimensions. This is the roughening transition point, analogous to roughening transitions found in other statistical systems. An example of the phenomenon is the divergent surface fluctuations of a magnetic domain wall, at the roughening transition point, found in the 3D Ising model. It is the existence of this phase transition in lattice QCD that prevents the extrapolation of strong-coupling lattice calculations into the weak-coupling regime.

Beyond the roughening transition, the width of the QCD flux tube must grow without limit as quark separation  $R$  increases. Lüscher, Münster, and Weisz suggested [1] that the two-Wilson loop correlation function in eq. (2.2) might be represented by the loop-loop correlation function  $G(H; C_1, C_2)$  of a Nambu-Goto string, which could be evaluated in the saddlepoint approximation. For this calculation it is convenient to choose  $C_1, C_2$  to be concentric circles in parallel planes, of radii  $R_1$  and  $R_2 > R_1$  respectively, separated by transverse distance  $H$  (as already noted, the loops used in eq. (2.2) need not be rectangular).

In ref. [1], the calculation of  $G(H; C_1, C_2)$  was done in flat space, and it was found that the cross-sectional area of the flux tube, evaluated in saddlepoint approximation,

grows logarithmically with quark separation. Of course, this result is not decisive for QCD, because the relationship of the QCD flux tube to the Nambu-Goto string is not entirely clear. However, from the AdS/CFT correspondence, we now understand the correct procedure (at strong couplings, large  $N$ , and  $D = 3$  dimensions) to be as follows: In an  $AdS_5 \times S_5$  background described by the black-hole metric [2–5] appropriate to  $QCD_3$ , we have

$$ds^2 = \alpha' \left[ \frac{U^2}{R^2} (f(U)dt^2 + dr^2 + dz^2 + r^2d\theta^2) + \frac{R^2}{U^2} \frac{dU^2}{f(U)} + R^2 d\Omega_5^2 \right], \quad (2.4)$$

with

$$f(U) = 1 - \frac{U_T^4}{U^4}, \quad R^2 = \sqrt{4\pi g N}. \quad (2.5)$$

The two loops shown in Fig. 1 are located at  $U = \infty$ , and at a fixed point on  $S_5$ . Each circular loop is centered at  $r = 0$  in a plane of constant  $z = z_1, z_2$  respectively, with  $H = |z_1 - z_2|$ . The  $QCD_3$  correlation function for two Wilson loops, appearing in eq. (2.2) is then determined by the loop-loop correlation function  $G(H; C_1, C_2)$  (i.e. the off-shell string propagator) in the  $AdS_5 \times S_5$  background, for the given loops at  $U = \infty$ .

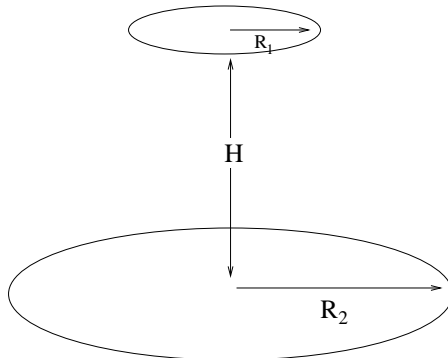


**Figure 1:** Loops  $C_1, C_2$  in the Wilson loop correlator  $G(H; C_1, C_2)$ .

Off-shell string propagators are complicated objects, even for strings on a flat background [13, 14], but it will be sufficient for our purposes to work in the saddle-point approximation. This means that

$$G(H; C_1, C_2) \approx \exp[-S(H; C_1, C_2)], \quad (2.6)$$

where  $S$  is the worldsheet action of the extremal surface in the AdS background, bounded by the two loops at  $U = \infty$ .<sup>3</sup> The saddle-point approximation has one important limitation: If  $H$  is too large, compared to the smaller of the two radii

<sup>3</sup>In the zero temperature case, and for  $R_1 = R_2$ , this propagator was computed by Zarembo [15] in the saddle-point approximation.

$R_1$ , then the minimal surface somewhere degenerates to a line. At that stage the semiclassical approximation has broken down, and a full quantum treatment of the string worldsheet is required, as discussed in ref. [4]. However, we will see that the small  $H$  behavior is sufficient to observe logarithmic broadening.

It is convenient to write the loop radii, transverse separation, and  $U_T$  as multiples of  $R$

$$R_1 = RL_1, \quad R_2 = RL_2, \quad H = Rh, \quad U_T = Rb \quad (2.7)$$

and also to rescale coordinates by the corresponding substitutions

$$U \rightarrow RU, \quad r \rightarrow Rr, \quad z \rightarrow Rz \quad (2.8)$$

We choose to parametrize surfaces by the rescaled metric coordinates  $r, \theta$ , and the symmetries of the problem allow us to consider surfaces with AdS coordinates  $U(r), z(r)$  independent of  $\theta$ . The worldsheet action in the  $AdS_5 \times S_5$  background is easily derived,

$$S = R^2 \int_{r_0}^{L_2} dr r U^2 \sqrt{F}, \quad (2.9)$$

with

$$F = 1 + \left( \frac{dz}{dr} \right)^2 + \frac{1}{U^4 - b^4} \left( \frac{dU}{dr} \right)^2. \quad (2.10)$$

The lower limit of integration in (2.9) is determined by the boundary conditions, as we will see in the next section. The action (2.9) does not contain the variable  $z$  explicitly, and hence we obtain the integral

$$\frac{dz}{dr} = \frac{q\sqrt{F}}{rU^2}. \quad (2.11)$$

Here  $q$  is an integration constant. By use of (2.10) we then obtain

$$\left( \frac{dz}{dr} \right)^2 = \frac{q^2 [1 + (U^4 - b^4)\phi^2]}{r^2 U^4 - q^2}, \quad (2.12)$$

where we introduced the notation

$$\phi = \frac{1}{U^4 - b^4} \frac{dU}{dr}. \quad (2.13)$$

The quantity  $F$  in eq. (2.10) can then be reexpressed as

$$F = \frac{r^2 U^4 (1 + (U^4 - b^4)\phi^2)}{r^2 U^4 - q^2}. \quad (2.14)$$

We also need the second derivative of  $z$ , which is most easily obtained from the hamiltonian  $H$  constructed from the action (2.9), with  $dH/dr = -\partial\mathcal{L}/\partial r$ . In this way we get

$$\frac{d}{dr} \left( \frac{rU^2}{\sqrt{F}} \right) = U^2 \sqrt{F}. \quad (2.15)$$

Inserting eq. (2.11) this leads to

$$\frac{d^2z}{dr^2} = -\frac{rU^4}{q^2} \left(\frac{dz}{dr}\right)^3. \quad (2.16)$$

We can then derive an equation of motion for the field  $\phi$ . Starting from eq. (2.15) we obtain after a tedious calculation

$$r\frac{d\phi}{dr} = \left(\frac{2r}{U} - \phi\right) \frac{r^2U^4 + q^2(U^4 - b^4)\phi^2}{r^2U^4 - q^2} - \phi^2 \left(\frac{2rb^4}{U} + (U^4 - b^4)\phi\right). \quad (2.17)$$

Together with eqs. (2.12) and (2.13) this constitutes the first-order saddle-point equations for the extremal surface, to be solved for  $U(r)$  and  $z(r)$  given appropriate 2-loop boundary conditions. Alternatively, one can use eq. (2.16) and

$$\left(\frac{dU}{dr}\right)^2 = (U^4 - b^4) \left[ \left(\frac{r^2U^4}{q^2} - 1\right) \left(\frac{dz}{dr}\right)^2 - 1 \right] \quad (2.18)$$

which follows from eqs. (2.12) and (2.13).

### 3. Numerical Solution for the Minimal Surface

It is possible to obtain two asymptotic solutions to the equations of motion derived above. The boundary of the world sheet corresponds to  $U = \infty$ . Let this occur at  $r = L$ , where  $L$  is to be identified with  $L_1$  or  $L_2$ . We find without difficulty that for  $U$  very large

$$U \approx \frac{1}{\sqrt{2L(L-r)}}. \quad (3.1)$$

It is, however, also possible for  $U$  to approach a constant value,  $U_0$  say, for  $r \rightarrow r_0$  in such a way that the derivative of  $U$  goes to infinity in this point. This behavior corresponds to

$$U \approx U_0 + \text{const.} \sqrt{r - r_0}. \quad (3.2)$$

Obviously this requires  $r > r_0$ .

The significance of these asymptotic forms can be appreciated by skipping ahead a little bit, and looking at a particular minimal surface, found by solving eqs. (2.12),(2.13),(2.17) numerically, for parameters  $L_1 = 2$ ,  $L_2 = 4$ ,  $h = 2.9$ ,  $b = 0.5$ . Solutions for  $U(r)$  (for  $U \leq 6$ ) and  $z(r)$  are shown in Figs. 2 and 3. By rotating these curves in  $\theta$  (i.e. around the  $U, z$  axes in the respective figures), one obtains a projection of the minimal surface in  $AdS_5$  onto the  $r\theta U$  and  $r\theta z$  hyperplanes.

Note that at both  $r \rightarrow L_1$  and  $r \rightarrow L_2$ , the slope  $dU/dr$  is positive, which can be immediately deduced from the asymptotic form (3.1). This means that  $U(r)$  is double-valued in some finite region  $r_0 < r < L_1$ , and it turns out that  $z(r)$  is also



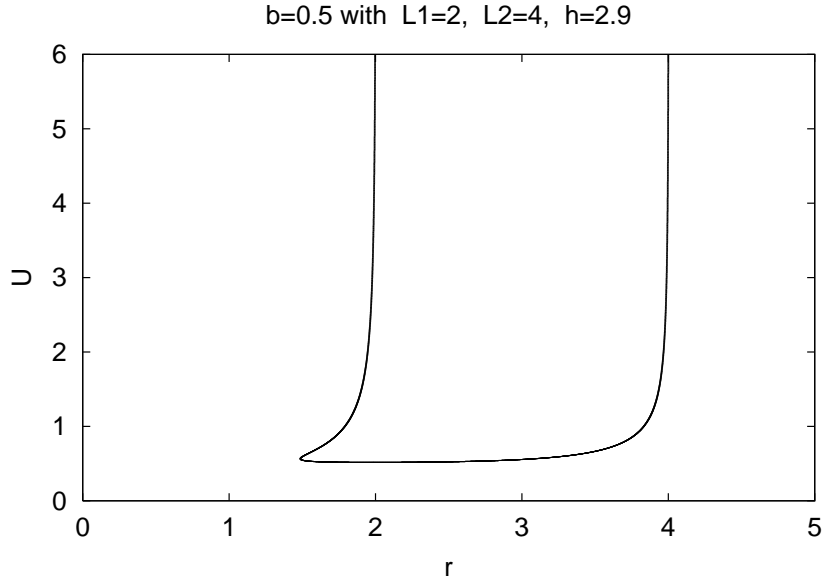


**Figure 2:** Profile of  $U(r)$ . The double valuedness of this function should be noticed.

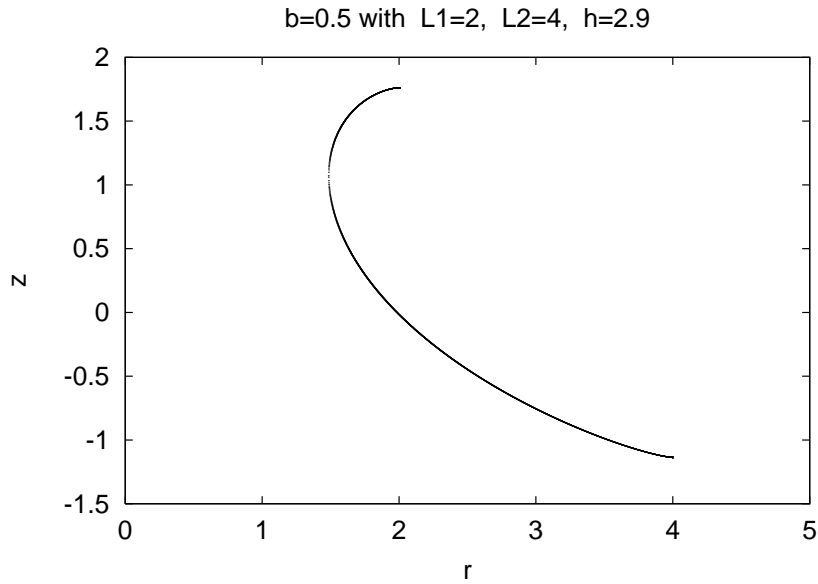


**Figure 3:** A profile of the function  $z(r)$ , which is also double valued.

double-valued in this range. At  $r = r_0$ , the slope  $dU/dr$  is infinite while  $U(r_0)$  is finite, and the form (3.2) applies.

Because of the double-valuedness of  $U(r)$  and  $z(r)$ , as well as for reasons of numerical stability, we have found it expedient to solve the equations for the minimal

surface numerically in the following way: We begin by noting that a solution of the equations of motion is completely determined by specifying the constant  $q > 0$ , and the coordinates  $(r_m, U_m, z_m)$  where  $U$  is a minimum ( $\phi = 0$ ). We can arbitrarily set  $z_m = 0$ , since only the difference  $h = |z(L_1) - z(L_2)|$  is relevant. Then we integrate the equations of motion from  $(r_m, U_m, z_m)$  in the positive  $r$  direction, to the limiting point  $r = L'_2$  where  $U \rightarrow \infty$ , and we denote  $z_2 = z(L'_2)$ .<sup>4</sup> In eq. (2.12) for  $dz/dr$ , there is a sign ambiguity in taking the square root (unless  $q = h = 0$ ). This is resolved by (arbitrarily) taking the slope to be negative (it does not pass through zero for  $r > r_m$ .) Next, again starting from the initial point  $(r_m, U_m, z_m)$ , we integrate in the negative  $r$ -direction until the point  $r_0, U_0, z_0$  is reached where  $dU/dr \rightarrow -\infty$  (also  $dz/dr \rightarrow -\infty$  if  $q \neq 0$ ). Finally, resetting  $dU/dr = +\infty$ , we integrate again in the positive direction from  $r_0, U_0, z_0$  to the limiting point  $r = L'_1, z = z_1$  where  $U = \infty$ . In this region the sign of  $dz/dr$  must be taken positive. Thus the integration is done separately in three regions  $[r_m, L'_2]$ ,  $[r_0, r_m]$ ,  $[r_0, L'_1]$ , and the double-valuedness problem is circumvented. It is then only necessary to choose parameters  $r_m, U_m, q$  such that  $L'_1 = L_1$ ,  $L'_2 = L_2$ ,  $h = |z_1 - z_2|$  for given  $L_1, L_2, h$ , which is achieved by a simple Newton-Raphson method. We note in passing that the example shown in Figs. 2, 3 was chosen so that the  $r_0 < L_1$  feature, and the double-valuedness of  $U(r), z(r)$  in the region  $r \in [r_0, L_1]$ , are very pronounced. In this example we had  $h = 2.9 > L_1 = 2$ . Generally, for the region of interest  $h \ll L_1$ , it is found that  $r_0$  is quite close to  $L_1$ , and the double-valuedness of  $U(r), z(r)$  is not so apparent.

Having obtained a numerical solution for the extremal surface bounding two loops, we can substitute the result back into the expression for the worldsheet action, eq. (2.9), which is then integrated numerically. Of course, the action is infinite if the loops are actually placed at  $U = \infty$ , so we regulate this infinity by placing the boundary loops at a finite  $U_{max} = 30$ . Then we can separate out an  $h$ -dependent area contribution

$$S[H; C_1, C_2] = R^2 \left( A_0[L_1, L_2] + A[h; L_1, L_2] \right) \quad (3.3)$$

where  $A[0; L_1, L_2] = 0$ . The term  $R^2 A_0[L_1, L_2]$  is the area of the string worldsheet at  $h = 0$ , which includes an irrelevant quark self-energy term, divergent as  $U_{max} \rightarrow \infty$ . We are mainly interested in the second,  $h$ -dependent term.

In flat space, the worldsheet action  $S[H, C_1, C_2]$  for a minimal surface between parallel concentric loops can be calculated analytically, and the result, for  $h \ll L_1 \ll L_2$ , is [1]

$$S_{flat}[H; C_1, C_2] = \sigma \pi R^2 (L_2^2 - L_1^2) + \frac{H^2}{d^2} \quad (3.4)$$

---

<sup>4</sup>Note that in practice, when we refer to the condition that  $U$  or its derivative is infinite, this is of course taken to mean that  $U$  or  $dU/dr$  exceeds some large finite bound.

where

$$d^2 = \frac{1}{\pi\sigma} \ln \frac{L_2}{L_1} \quad (3.5)$$

with  $\sigma$  the string tension. The logarithmic dependence of  $d^2$  on  $L_2$  is evidence, in the saddle-point approximation, of logarithmic broadening of the flux tube. Lüscher, Münster, and Weisz also argued in ref. [1] that this logarithmic dependence on  $L_2$  holds beyond the saddle-point approximation, in the  $L_1 \rightarrow 0$  limit, where the factor of  $L_1$  in eq. (3.5) is replaced by a short-wavelength cutoff  $\lambda$ .

To check for this logarithmic broadening in the AdS/CFT correspondence, we first fit the  $h$ -dependent part of the worldsheet action,  $A[h; L_1, L_2]$ , to a parabola

$$A[h; L_1, L_2] \sim \frac{h^2}{d^2} \quad (3.6)$$

so that, for small  $h \ll L_1$  ( $H \ll R_1$ ), we have

$$G[H; C_1, C_2] \sim \exp[-H^2/d^2] \quad (3.7)$$

where  $d$  will depend on  $L_1, L_2$ . Of course this parabolic form will not hold for large  $h$ , where we would expect not a gaussian but rather a simple exponential falloff for the loop-loop correlation function

$$G[H; C_1, C_2] \sim \exp[-m_G H] \quad (3.8)$$

where  $m_G$  is the lowest-lying glueball state, corresponding to a dilaton exchange in  $AdS_5 \times S_5$ . This asymptotic behavior cannot be accurately obtained in the saddle-point approximation, which breaks down for  $h \gg L_1$ , but even in the saddle-point approximation there is a deviation from gaussian falloff at large enough  $h$ . Therefore, in fitting  $A[h; L_1, L_2]$  to a parabola, we obtain  $d$  from a fit in the restricted range of  $h \in [0, L_1/4]$ .<sup>5</sup>

At small  $h$ , our numerical solutions for  $A[h; L_1, L_2]$  are fit very accurately by a parabola, as shown in Fig. 4, where we plot our data for  $A[h; 4, 12]$  (crosses) versus a parabola (solid line) with  $d = 1.492$ . In general we can extract  $d$  from the numerical solution to at least three digit accuracy. For larger  $h \gg L_1/4$ , the worldsheet action goes over to a linear increase with  $h$ , as shown in Fig. 5 (the slope is proportional to  $L_1$ ). At large enough  $h$  the saddle-point equations have no solution, as already noted above.

In AdS/CFT, the string tension at strong coupling is given by

$$\sigma = \frac{b^2}{2\pi} = \frac{U_T^2}{2\pi R^2} \quad (3.9)$$

---

<sup>5</sup>All fits were obtained using the data fitting capabilities of the GNU PLOT software package.

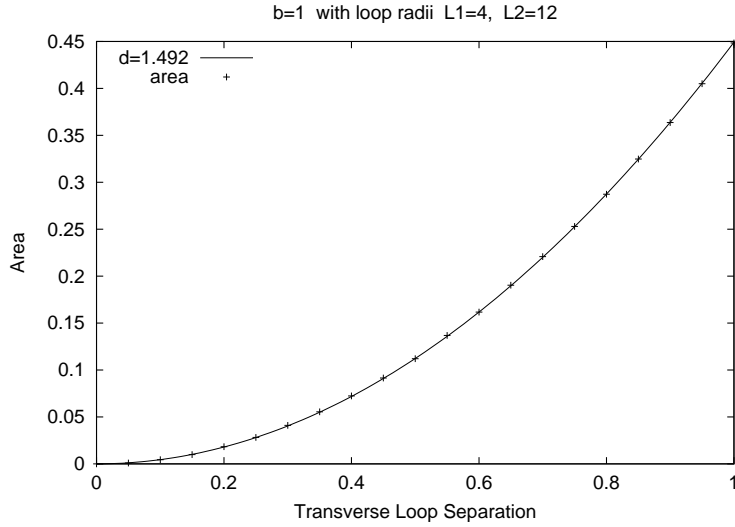


**Figure 4:** The  $h$ -dependent part of the worldsheet area  $A[h; L_1, L_2]$  (denoted “area”) at fixed radii, and the best parabolic fit. Note that  $A[h; L_1, L_2]$  is the worldsheet area/ $R^2$  with a subtraction, so as to equal zero at  $h = 0$ .

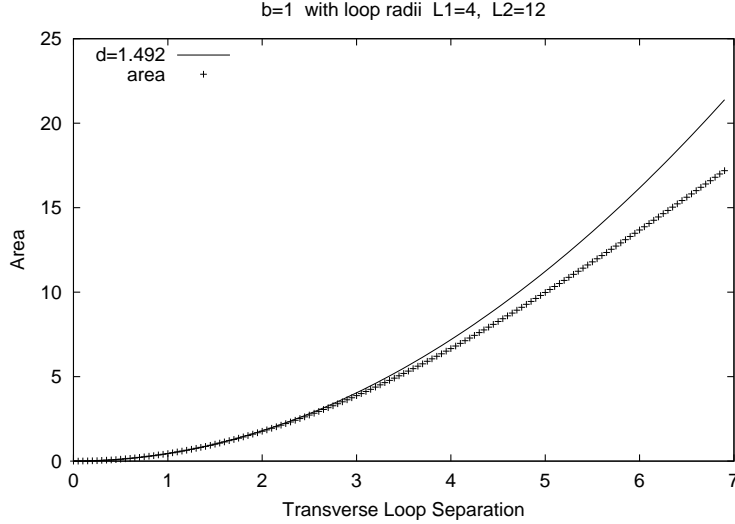


**Figure 5:** The  $h$ -dependent area term  $A[h; L_1, L_2]$  (denoted “area”) at larger values of  $h$ . The parabolic fit obtained at  $h \in [0, 1]$  is also displayed. For  $h > 3.5$  the behavior becomes linear in  $h$ .

Therefore, if the Lüscher, Münster, and Weisz formula (3.5) holds for the flux tube in the AdS/CFT correspondence, then one expects

$$d = \frac{1}{b} \left[ 2 \ln \frac{L_2}{L_1} \right]^{1/2} \quad (3.10)$$

In Fig. 6 we plot the tube radius  $d$  vs. the ratio  $L_1/L_2$  for a variety of  $L_1, L_2$  values, at fixed finite temperature  $b = 1$ .<sup>6</sup> It appears that the numerical solution for  $d$  depends only on the ratio  $L_1/L_2$ , and fits eq. (3.10) quite well. We are therefore justified in concluding that the cross-section of the  $QCD_3$  flux tube, as probed by the smaller loop of radius  $L_1$ , broadens logarithmically with  $L_2/L_1$  in the strong-coupling AdS/CFT correspondence. There is then no reason to expect, in the AdS/CFT correspondence, a roughening transition separating strong and weak-coupling phases.

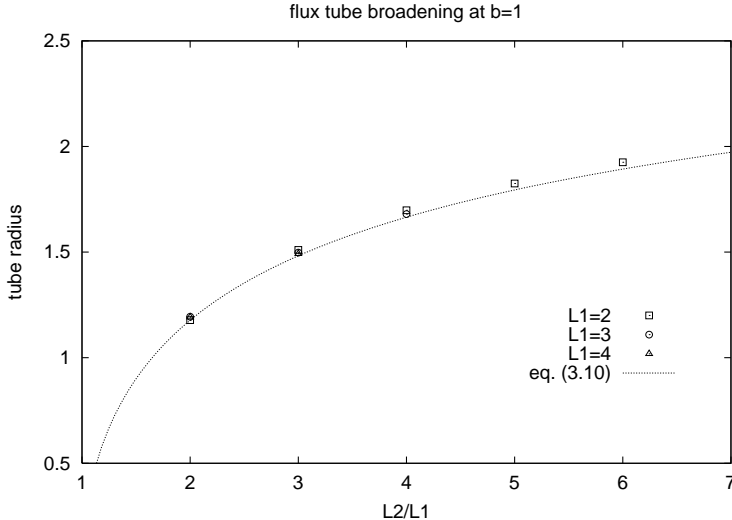


**Figure 6:** The tube radius  $d$  as a function of  $L_1/L_2$  with fixed temperature  $b = 1$ .

Next we investigate the variation of  $d$  with the temperature parameter  $b$ . According to eq. (3.10),  $d$  varies inversely with  $b$ , but this equation cannot possibly be right in the  $b \rightarrow 0$  limit, where supersymmetry is restored and the confining flux tube disappears. For fixed  $L_1 = 2$ ,  $L_2 = 4$ , the variation of  $d$  with  $b$  is shown in Fig. 7. The solid line is eq. (3.10), which again fits the numerical solution very well at these values of  $L_1$ ,  $L_2$  for  $b \geq 1$ . As  $b \rightarrow 0$ , however,  $d$  goes to a finite constant.

The result that  $d$  ceases to depend on the logarithm of  $L_2/L_1$  in the zero temperature case can be understood from a straightforward generalization of the work by Zarembo [15] (where he studied the case  $L_1 = L_2$ ) to the case where  $L_1$  and  $L_2$  are different. In the  $L_1 \neq L_2$  case one finds, after expanding the action to lowest order in  $h^2$  and dropping the perimeter term [16]

$$S \approx R^2 G(k_0) + \frac{G'(k_0)}{2(1 - R_1^2/R_2^2)F'(k_0)} \frac{H^2}{L_2^2}, \quad (3.11)$$

<sup>6</sup>Numerical instability limits our choice of  $L_1$  and  $L_2$ , since the allowable numerical error required for results of fixed accuracy decreases exponentially as  $L_2$  increases.

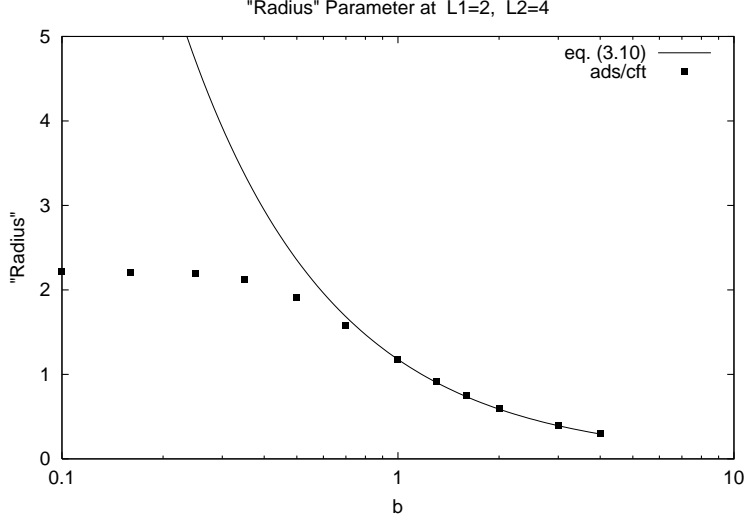


**Figure 7:** Variation of the “radius”  $d$  with the temperature.

where  $k_0$  is determined in terms of the ratio  $R_2/R_1$  by the transcendental equation

$$F(k_0) = \frac{k_0}{2} \int_0^1 du \frac{\sqrt{\sqrt{1 + 4k_0^2(1-u)} - 1}}{\sqrt{u(2k_0^2 + 1 - \sqrt{1 + 4k_0^2(1-u)})}(1 + 4k_0^2(1-u))} = \frac{1}{2} \ln \frac{R_2}{R_1}. \quad (3.12)$$

In eq. (3.11) the quantity  $F'(k_0)$  is the derivative of the function  $F$ , and  $G'(k_0)$  is the derivative of the function

$$G(k_0) = -\frac{2\alpha}{\sqrt{\alpha-1}} \int_0^{\pi/2} \frac{d\psi}{1 + \alpha \sin^2 \psi + \sqrt{1 + \alpha \sin^2 \psi}}, \quad \alpha = \frac{1 + 2k_0^2 + \sqrt{1 + 4k_0^2}}{2k_0^2}. \quad (3.13)$$

To compare eq. (3.11) with our numerical results we take  $R_2/R_1 = 2$ , corresponding to  $k_0 \approx 2.53$ , obtained by solving (3.12). We then evaluate the derivatives entering in eq. (3.11) numerically and obtain

$$S(H) \approx 3.094 \left( \frac{H}{L_2} \right)^2, \quad (3.14)$$

in good agreement with the result shown in Fig. 7. In this case the width is given by

$$d \approx \frac{L_2}{\sqrt{3.1}} \quad \text{for} \quad \frac{L_2}{L_1} = 2. \quad (3.15)$$

For different ratios  $L_1/L_2$  the transcendental equation (3.12) should again be solved, the derivatives of  $F$  and  $G$  be computed and inserted in (3.11). The coefficient of  $H^2/L_2^2$  depends on  $L_1/L_2$ , so there is no universality in the coefficient. As an example

illustrating this, we can take  $L_2/L_1 = 2.7$  (corresponding to  $k_0 \approx 0.70$ ), which gives  $S(H) \approx 0.61H^2/L_2^2$ . The variation of the coefficient of  $H^2/L_2^2$  from  $L_2/L_1 = 2.7$  to  $L_2/L_1 = 2$  is  $0.61/3.1 \approx 0.20$ . However, the corresponding logarithms would vary like  $\ln 2/\ln 2.7 \approx 0.70$ , so the decrease of the coefficient with the ratio  $L_2/L_1$  cannot be explained by a logarithmic width as in the finite temperature case. It is also quite clear from Fig. 7 that the logarithmic fit fails for small temperatures, and  $d$  does not have the interpretation of the radius of a flux tube. This is quite satisfactory, since there does not exist any flux tube at zero temperature due to the vanishing string tension.

The parameter  $d$  at  $b = 0$  can be extracted just as in the finite temperature case. In Fig. 8 we plot  $d$  vs.  $L_2$ , with  $L_1/L_2 = \frac{1}{2}$  kept fixed. We see that the values obtained numerically for  $d$  are in excellent agreement with the expected behavior (3.15).<sup>7</sup>

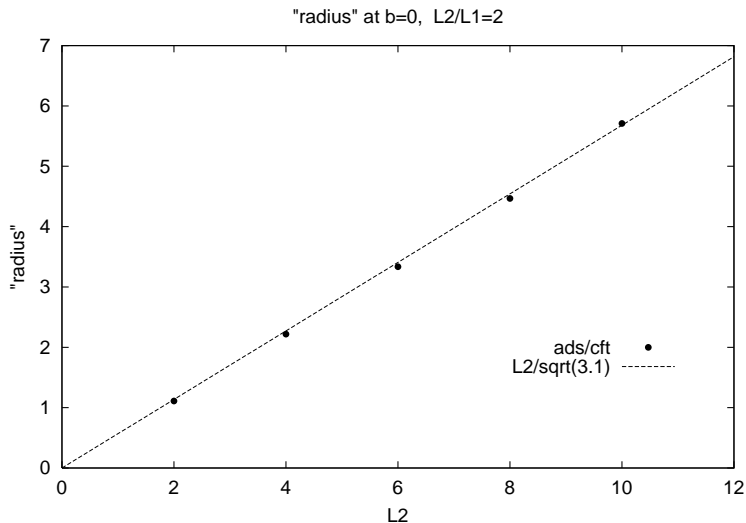


**Figure 8:** Zero temperature behavior of the radial parameter  $d$ .

## 4. Analytic Approximation

From the numerical result we see that the behavior of  $U$  is characterized by a “plateau” where  $U$  is approximately a constant. If we now make the somewhat prim-

<sup>7</sup>Correlation between large and small loops in the zero temperature theory has also been discussed by Berenstein et al. [17]. In that reference, the correlation is calculated by running propagators (dilaton, graviton,...) between the small loop and points on the classical worldsheet of the large loop. The relation of their result to ours is not entirely direct, since for  $H \ll R_2$  and  $R_1 \rightarrow 0$  one has to sum over propagators for many excitations, and it is also not clear if, in this limit, the quantum fluctuations of the large loop worldsheet can be neglected.

itive approximation that  $U \approx U_{\min}$  and the derivative  $dU/dr \approx 0$  on the plateau, then from eqs. (2.13) and (2.12) we obtain for the height  $h$

$$\begin{aligned} h &= q \int_{\text{whole range of } r} dr \sqrt{\frac{1 + (U^4 - b^4)\phi^2}{r^2 U^4 - q^2}} \approx q \int_{L_1}^{L_2} dr \frac{1}{\sqrt{r^2 U_{\min}^4 - q^2}} \\ &= \frac{q}{U_{\min}^2} \ln \frac{L_2 + \sqrt{L_2^2 - q^2/U_{\min}^4}}{L_1 + \sqrt{L_1^2 - q^2/U_{\min}^4}}. \end{aligned} \quad (4.1)$$

In the second step we have ignored the contributions to the integral away from the plateau. These are essentially the irrelevant infinite self energy contributions. Further, we used that on the plateau one has that the quantity

$$P \equiv (U^4 - b^4)\phi^2 = \left(\frac{dU}{dr}\right)^2 \frac{1}{U^4 - b^4} \quad (4.2)$$

is very small relative to one. This can be seen from the numerical results, which show that relative to one the quantity  $P$  is at most of the order of a few per cent in a range going from slightly above  $L_1$  to slightly below  $L_2$ . Near the minimum,  $P$  behaves like

$$P \approx \frac{1}{2U_{\min}^3} \frac{d^2U}{dr^2}. \quad (4.3)$$

On the plateau the second derivative of  $U$  is very small, as can be seen from the numerical results. For  $L_1$  and  $L_2$  sufficiently large relative to  $q/U_{\min}^2$  we obtain

$$\frac{U_{\min}^2}{q} \approx \frac{1}{h} \ln \frac{L_2}{L_1}. \quad (4.4)$$

Since  $U_{\min}$  approaches  $b$  with small exponential corrections for large  $L_1$  the quantity  $q/U_{\min}^2$  is very close to  $q/b^2$ .

In the same approximation as in (4.1) we obtain for the action from eqs.(2.9) and (2.14)

$$\begin{aligned} S &= R^2 \int_{\text{whole range of } r} dr r^2 U^4 \sqrt{\frac{1 + (U^4 - b^4)\phi^2}{r^2 U^4 - q^2}} \approx R^2 U_{\min}^4 \int_{L_1}^{L_2} dr \frac{r^2}{\sqrt{r^2 U_{\min}^4 - q^2}} \\ &= \frac{1}{2} R^2 U_{\min}^2 \left[ r \sqrt{r^2 - q^2/U_{\min}^4} + \frac{q^2}{U_{\min}^4} \ln \left( r + \sqrt{r^2 - q^2/U_{\min}^4} \right) \right]_{L_1}^{L_2}. \end{aligned} \quad (4.5)$$

Using (4.4) in this we obtain

$$S \approx \frac{1}{2} U_{\min}^2 R^2 \left( (L_2^2 - L_1^2) + \frac{h^2}{\ln(L_2/L_1)} \right) \approx \frac{1}{2} b^2 \left( (R_2^2 - R_1^2) + \frac{H^2}{\ln(L_2/L_1)} \right). \quad (4.6)$$

Therefore  $\exp(-S)$  is a Gaussian in  $h$  with a logarithmic width, as we have seen from the numerical results. The above expression for  $S$  is identical to the flat space result, eqs. (3.4) and (3.5), with  $\sigma$  replaced by the AdS/CFT string tension in eq. (3.9).



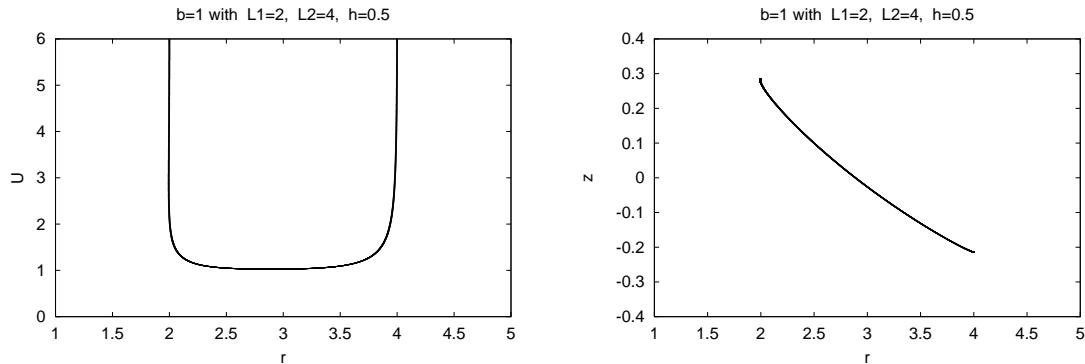


**Figure 9:** Profiles of  $U(r)$  and  $z(r)$  for finite temperature.

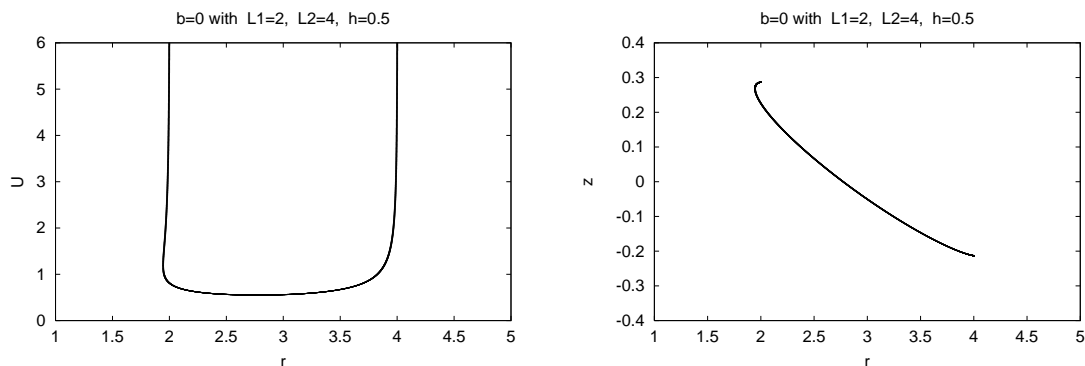


**Figure 10:** Profiles of  $U(r)$  and  $z(r)$  for zero temperature. Otherwise the parameters are the same as used in Fig. 9 in the finite temperature case.

In Figs. 9 and 10 we have shown the behaviors of  $U$  in two cases with the same  $L_1$ ,  $L_2$  and  $h$ , but in Fig. 9 the temperature is finite, whereas it is zero in Fig. 10. It is seen that the two cases superficially look very similar. In spite of this, there is only logarithmic broadening in the first case. Thus the AdS/CFT correspondence is able, by subtle effects, to distinguish the two cases.

If we turn to the approximations given in Eqs. (4.1)-(4.5) it is easy to see that they break down in the zero temperature case: There is still a plateau, but of course the string tension disappears: For  $b = 0$  we have  $U_{\min}^2 \propto 1/L^2 \rightarrow 0$ , as shown in ref. [2]. The logarithmic term on the right hand side of Eq. (4.5) is therefore multiplied by an overall factor which vanishes in the limit  $L \rightarrow \infty$ . Since the derivation of the analytic approximation is only asymptotic, subdominant terms have already been disregarded, and hence the term of order  $1/L_1^2 \ln(L_2/L_1)$  should also be disregarded. We therefore have the satisfactory situation that in the supersymmetric case the logarithmic broadening disappears.

## 5. Four dimensional QCD

So far we have discussed  $QCD_3$ . However it is not difficult to extend the method to four dimensional  $QCD$ . Making rescalings similar to the previous ones we obtain the action

$$S \propto \int dr rU^3 \sqrt{1 + z'^2 + \frac{U'^2}{U^3 - b^2}}. \quad (5.1)$$

Here a prime denotes differentiation with respect to  $r$ . Proceeding as before we get the equations of motion

$$z'' = -\frac{rU^6}{q^2} z'^3, \quad (5.2)$$

where  $q$  is again a constant of integration, and

$$U'^2 = (U^3 - b^3) \left( \frac{r^2 U^6}{q^2} z'^2 - z'^2 - 1 \right). \quad (5.3)$$

These equations are very similar to the three dimensional ones. We have checked that the profiles for  $U$  and  $z$  are extremely similar in  $QCD_3$  and  $QCD_4$ , with plateaus in the  $U(r)$  profiles. The analytic approximation in the previous section can therefore be performed as before, leading again to a logarithmic broadening of the string. It is easy to show that the asymptotic result (3.2) remains valid, while eq. (3.1) is replaced by

$$U \approx \sqrt{\frac{2}{5L}} \frac{1}{L - r} \quad (5.4)$$

leading to a somewhat faster approach to infinity at the end points.

## 6. Conclusions

We have studied the broadening of the  $QCD_3$  flux tube, as probed by a Wilson loop whose extension is small compared to the quark separation, in the AdS/CFT correspondence at strong couplings. It is found that the cross-sectional area of flux tube, as measured by the loop probe, grows logarithmically with quark separation, in the manner first suggested in ref. [1]. Thus there is no roughening phase transition, as exists in lattice gauge theory, to frustrate the extrapolation of strong coupling results to weaker couplings. Possibly this extrapolation could be carried out by resummation methods. We have also found that in the zero-temperature limit, our results are consistent with the absence of a flux tube, and no logarithmic broadening of the field-strength distribution in a transverse direction.

We have not yet answered the question: “How thick are chromo-electric flux tubes?” This is because the thickness, as probed by a small Wilson loop, also depends logarithmically on the radius of the small loop, as seen in eq. (3.10). However, the finite temperature formulation only resembles  $QCD_3$  at length scales greater than

the inverse temperature, which serves as a kind of short distance cutoff. Questions pertaining to  $QCD_3$  can only be addressed, in the finite-temperature AdS/CFT correspondence, in terms of observables whose relevant length scales are larger than this effective cutoff. From this point of view the smallest loop probe that we can use, and still be talking about  $QCD_3$ , would have a radius  $R_1 \equiv RL_1$  on the order of the inverse temperature  $R_1 \sim 1/T = \pi R/b$ , in which case the diameter of the flux tube associated with a circular loop of radius  $R_2$  would be

$$d \approx \frac{1}{b} \left[ 2 \ln \left( \frac{bR_2}{\pi R} \right) \right]^{1/2} \quad (6.1)$$

Of course, whether or not it is relevant to  $QCD_3$ , the behavior of  $d$  in the  $L_1 \rightarrow 0$  limit is well defined in the AdS/CFT correspondence. In this limit the saddle-point approximation that we have been using certainly breaks down, and it is necessary to compute the full off-shell string propagator in  $AdS_5 \times S_5$  between a large loop and a second loop shrunk to a point. It would be interesting to have further information about the behavior of  $d$  in this limit.

## Acknowledgments

J.G. acknowledges the financial support of MaPhySto, Centre for Mathematical Physics and Stochastics, funded by the Danish National Research Foundation. J.G.'s research is also supported in part by the U.S. Department of Energy under Grant No. DE-FG03-92ER40711.

## References

- [1] M. Lüscher, G. Münster, and P. Weisz, Nucl. Phys. B180 (1981) 1.
- [2] J. Maldacena, Adv. Theor. Math. Phys. 2 (1998) 231, hep-th/9711200.
- [3] E. Witten, Adv. Theor. Math. Phys. 2 (1998) 505, hep-th/9803131.
- [4] D. J. Gross and H. Ooguri, Phys. Rev. D58 (1998) 106002, hep-th/9805129.
- [5] A. Brandhuber, N. Itzhaki, J. Sonnenschein, and S. Yankielowicz, J. High Energy Phys. 9806 (1998) 001, hep-th/9803263; Phys. Lett. B434 (1998) 36, hep-th/9803137; S-J. Rey and J-T. Yee, hep-th/9803001; S-J. Rey, S. Theisen and J-T. Yee, Nucl. Phys. B527 (1998) 171, hep-th/9806125; J. Greensite and P. Olesen, J. High Energy Phys. 9808 (1998) 009, hep-th/9806235.
- [6] J. Greensite and P. Olesen, J. High Energy Phys. 9904 (1999) 001, hep-th/9901057.
- [7] Y. Kinar, E. Schreiber, J. Sonnenschein, and N. Weiss, hep-th/9911123.

- [8] N. Drukker, D. J. Gross, and A. Tseytlin, J. High Energy Phys. 0004 (2000) 021, hep-th/0001204;  
S. Förste, D. Ghoshal and S. Theisen, J. High Energy Phys. 9908 (1999) 013, hep-th/9903042.
- [9] O. Alvarez, Phys. Rev. D24 (1981) 440.
- [10] M. Caselle, F. Gliozzi, U. Magnea and S. Vinti, Nuc. Phys. B460 (1996) 397, hep-lat/9510019.
- [11] G. S. Bali, C. Schlichter, and K. Schilling, Phys. Rev. D51 (1995) 5165.
- [12] A. Tseytlin, Talk given at the Triangle meeting, Copenhagen, June 2000.
- [13] A. Cohen, G. Moore, P. Nelson, and J. Polchinski, Nucl. Phys. B267 (1986) 143.
- [14] S. Chaudhuri and E. Novak, hep-th/0002046.
- [15] K. Zarembo, Phys. Lett. B459 (1999) 527, hep-th/9904149.
- [16] P. Olesen and K. Zarembo, hep-th/0009210.
- [17] D. Berenstein, R. Corrado, W. Fischler, and J. Maldacena, Phys. Rev. D59 (1999) 105023, hep-th/9809188.